Eur. Phys. J. D **19**, 25–29 (2002)
DOI: 10.1140/epjd/e20020051

THE EUROPEAN PHYSICAL JOURNAL D
EDP Sciences

Hyperfine structure and isotope shift measurements on $4d^{10}\ ^1S_0 \rightarrow 4d^9\ 5p\ J = 1$ transitions in Pd I using deep-UV cw laser spectroscopy

E.J. van Duijn[a], S. Witte, R. Zinkstok, and W. Hogervorst

Atomic Physics Group, Laser Centre Vrije Universiteit, De Boelelaan 1081, 1081HV Amsterdam, The Netherlands

Received 3 October 2001

Abstract. The $4d^{10}\ ^1S_0$ ground-state transitions to the $4d^9\ 5p$ configuration of palladium (Pd) have been studied. For this purpose, a tunable, single-mode, deep-UV cw laser has been built to generate the sum frequency of a frequency-doubled Ti:S laser with a second Ti:S laser. The produced wavelengths range from 244 to 276 nm. From the measured spectra the frequency splitting due to hyperfine structure and isotope shift, the hyperfine structure A and B constants and the lifetimes of the states have been extracted.

PACS. 31.30.Gs Hyperfine interactions and isotope effects, Jahn-Teller effect – 32.30.Jc Visible and ultraviolet spectra – 42.62.Fi Laser spectroscopy

1 Introduction

Data on isotope shifts (IS) and hyperfine structure (HFS) in ground-state transitions to the first excited states are accurately known for nearly all elements occurring in nature. One of the few exceptions is palladium (Pd I) for which – to the authors knowledge – these data are missing or have a large uncertainty.

The $4d^9\ 5p$ configuration of Pd I contains the first excited states accessible from the $4d^{10}\ ^1S_0$ ground state. These are the $4d^9 5p\ ^3P_1$ state at 36 180.678 cm^{-1}, the $4d^9 5p\ ^3D_1$ state at 40 368.795 cm^{-1} and the $4d^9 5p\ ^1P_1$ state at 40 838.874 cm^{-1} [1]. It is the relatively high excitation energy in combination with the difficulty to generate narrow-band cw radiation at this wavelength, and the relatively small IS and HFS in Pd I that thus far has hampered a detailed investigation using laser-induced fluorescence spectroscopy (LIF).

In various studies measurements of the HFS and IS in Pd I on other energy levels have been presented [1–4]. Only in references [1,5] some HFS and IS data on the transitions reported in this paper are given. In reference [1] a Fourier transform spectrometer was used, while in reference [5] the level crossing technique was applied. Furthermore, none of these studies were done using LIF under the Doppler-free conditions of an atomic beam.

In this paper we present the experimental results on HFS and IS measurements in the transitions from the ground state to the states in the $4d^9\ 5p$ configuration mentioned above. The measurements are performed using a tunable, deep-UV cw laser system with a linewidth $\Gamma \approx 3$ MHz. Due to this high resolution, much improved hyperfine-structure data on the $4d^9 5p\ ^3P_1$ have been deduced, while isotope shift and hyperfine structure of the other states have been accurately measured for the first time.

2 Experimental method and setup

2.1 Laser system

In order to study the deep-UV transitions, a tunable cw laser operating at wavelengths ranging from 244 to 276 nm has been developed (Fig. 1). For this purpose, a cw Ti:sapphire laser pumped by a 10 W Spectra Physics Millenia laser is frequency doubled in an external enhancement cavity (EEC) using an LBO crystal Brewster cut for the fundamental wavelength ($\theta = 90°$ and $\phi = 33.7°$). To keep the cavity in resonance with the laser light, the Hänsch-Couillaud locking technique [6] is used. With 1.5 W of fundamental (IR) light, about 600 mW of second harmonic (UV) light is produced. To reach the deep-UV wavelength the UV light from the EEC is sum-frequency mixed with the light from a second, similar Ti:S laser by overlapping the waists of both beams in a BBO crystal, using a telescope system. To generate light at 276 nm, a BBO crystal cut at $\theta = 41.1°$ is used, while for the generation of 247 and 244 nm light a crystal cut at $\theta = 55°$ is more appropriate. To realize type I phase matching, the polarization of the UV beam is rotated over 90° by a $\lambda/2$

[a] e-mail: ejvduijn@nat.vu.nl

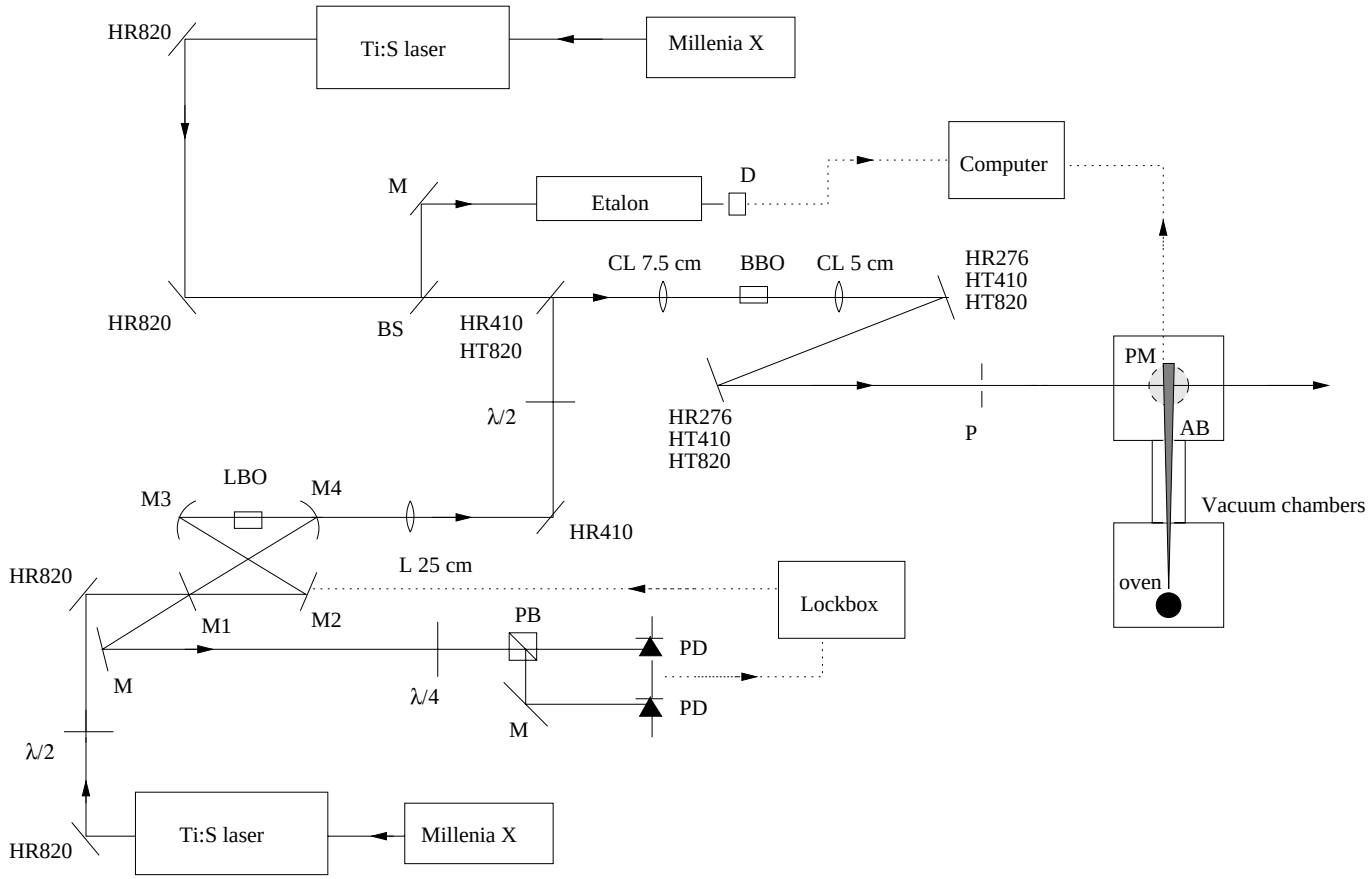

Fig. 1. Overview of the experimental setup used for HFS and IS measurements on Pd I at 276 nm. A Millenia pumped cw Ti:S laser at $\lambda = 822$ nm is frequency doubled in an external enhancement cavity doubler consisting of mirrors M1–M4 using an LBO crystal. The cavity is locked to the fundamental using a Hänsch-Couillaud locking technique which employs a quarter-wave plate ($\lambda/4$), a polarizing beamsplitter (PB) and two photodiodes (PD). The $\lambda = 411$ nm beam is combined with the output beam of a second Millenia pumped Ti:S laser operating at $\lambda = 843$ nm in a BBO crystal placed in the focus of a telescope consisting of two cylindrical lenses (CL). In the BBO crystal the sum frequency at $\lambda = 276$ nm is generated. The polarization of the frequency doubled beam is rotated over 90° by a half-wave plate ($\lambda/2$) in order to achieve type I phase-matching. The 276 nm beam passes through a pinhole (P), after which it intersects an atomic beam (AB) of Pd. The laser-induced fluorescence is monitored by a photomultiplier (PM) placed directly above the intersection of laser and atomic beam. An etalon and a detector (D) are used as a reference for the relative frequency during measurements.

plate. In the sum frequency mixing process ~ 10 μW of 276 nm (deep-UV) laser light is produced.

Behind the telescope two mirrors are placed that reflect the deep-UV light, but transmit most of the UV and IR light still present in the output beam. The deep-UV beam then perpendicularly intersects an atomic beam of Pd, and is back-reflected to enhance the signal to noise ratio. The linewidth of the deep-UV light is equal to the sum of the linewidths of the UV and IR beams, which are about 2 and 1 MHz respectively. Thus the linewidth of the deep-UV light is about 3 MHz.

Frequency scanning is done by tuning the Ti:S laser that provides the IR beam in the sum-frequency mixing process. Frequency scans are calibrated by sending a small fraction of the IR light through a high-finesse confocal etalon with a free spectral range of 150 MHz, providing frequency markers. By monitoring the etalon output and the photomultiplier signal simultaneously during a scan, the frequency intervals between measured spectral lines can be determined with an error smaller than 0.3 MHz.

2.2 Atomic beam, vacuum system and data processing

The atomic beam is produced by heating a small sample of Pd placed inside a tantalum oven. The oven is heated to a temperature of about 1 500 °C by electron bombardment from a nearby tungsten wire, heated with a large current (≈ 13 A at ≈ 30 V). At this temperature the vapor pressure of Pd is high enough to produce an atomic beam of sufficient intensity, leaving the oven through a small hole. About 30 cm downstream the beam passes through a diaphragm, 3 mm in diameter, after which a highly collimated beam remains. From the beam divergence the residual Doppler broadening in the measured spectral lines can be estimated to be 19 MHz.

The vacuum system contains two compartments connected by a valve (Fig. 1). The first compartment contains the oven where the atomic beam is produced, while in the second compartment the LIF measurements are performed. The deep-UV laser beam passes through this second compartment, where it intersects the atomic beam at an angle of 90° in order to minimize Doppler broadening and shift. Directly above the point where the beams intersect a photomultiplier tube (PMT) is mounted. The fluorescence spot is imaged with a lens system on the PMT. To minimize detection of stray light and radiation from the oven, spatial filtering in combination with a deep-UV filter is employed. The photomultiplier signal is fed through a discriminator to a counter, connected to a computer for analysis.

Finally, the absolute wavelength of the lines is measured with a systematic error below 100 MHz ($0.003\,\mathrm{cm}^{-1}$) using an ATOS LM-007 lambdameter.

3 The $4d^{10}\ {}^1S_0 \rightarrow 4d^9 5p$ transitions

Natural palladium has six different stable isotopes, ^{102}Pd, ^{104}Pd, ^{105}Pd, ^{106}Pd, ^{108}Pd and ^{110}Pd, with abundances of respectively 1.02%, 11.14%, 22.33%, 27.33%, 26.47%, and 11.74%. All isotopes have nuclear spin $I = 0$, except for ^{105}Pd, which has $I = 5/2$. Consequently, hyperfine structure is present only in ^{105}Pd, where three separate transitions are expected corresponding to the hyperfine splitting of the $J = 1$ upper state according to $F = I+J = 7/2,\ 5/2,\ 3/2$. The spectrum of a $4d^{10}\ {}^1S_0 \rightarrow 4d^9 5p$ ($J = 1$) transition is therefore expected to show eight peaks, one for each isotope plus three for ^{105}Pd. An estimate for the magnitude of the isotope shift in palladium can be made using the expression for the total mass shift, involving both normal and specific mass shift [7]:

$$\Delta\nu = K\frac{M - M'}{MM'} \tag{1}$$

where K is a constant and M and M' are the masses of two neighbouring isotopes. This results in the case of Pd in shifts of the order of 50−100 MHz between neighbouring isotopes. The field shift, which is caused by the charge distribution in the nucleus, is expected to be small because the transitions under consideration only involve an electron being excited from a d to a p orbital, for which the spatial overlap with the nucleus is small.

Two contributions to the HFS are distinguished. Firstly, when the nucleus of an atom has a nonzero spin quantum number I, the interaction of the nuclear magnetic moment μ_n with the magnetic field $\mathbf{B}_{\mathrm{el}}$ caused by the electrons moving around the nucleus has to be taken into account. Secondly, there is the interaction between the nuclear electric quadrupole moment $\mathbf{Q}_n$ and the electric field gradient $\mathbf{q}$ produced by the electrons. These give rise to two additional terms in the atom's Hamiltonian of the form:

$$H_{\mathrm{hfs}} = -\boldsymbol{\mu}_n \cdot \mathbf{B}_{\mathrm{el}} + \mathbf{Q}_n \cdot \mathbf{q}. \tag{2}$$

Because the magnitude of these terms is small compared to the other terms in the atomic Hamiltonian, the resulting energy contributions can be calculated in first order perturbation theory. This leads to [8]:

$$\Delta E = \frac{A}{2}K + \frac{B}{4}\frac{\frac{3}{2}K(K+1) - 2I(I+1)J(J+1)}{I(2I-1)J(2J-1)}, \tag{3}$$

where $K = F(F+1) - J(J+1) - I(I+1)$. A and B represent the magnetic dipole and the electric quadrupole constants respectively. For the $4d^9 5p\ {}^3P_1$ state, the hyperfine splitting of ^{105}Pd was measured by Liening [5] to be 319 and 543 MHz for the 5/2−7/2 and 3/2−5/2 splitting respectively.

From equation (3), the following equations can be derived for the energy differences between the hyperfine levels, involving only the hyperfine structure A and B constants:

$$\begin{aligned} E_{F=7/2} - E_{F=5/2} &= \frac{7}{2}A + \frac{21}{20}B \\ E_{F=5/2} - E_{F=3/2} &= \frac{5}{2}A - \frac{3}{2}B \end{aligned} \tag{4}$$

A and B then follow from these equations and the measured energy splittings.

A hyperfine energy level is characterized by a wave function $|J\ I\ F\rangle$. The probability for the transition from a state $|J'\ I'\ F'\rangle$ to a state $|J\ I\ F\rangle$ is given by the square of the matrix element for an electric dipole transition. This matrix element is (see *e.g.* [9]):

$$\begin{aligned} \langle JIF\|Q_1^{\mathrm{el}}\|J'I'F'\rangle = (-1)^{J+I+F'+1}\sqrt{(2F+1)(2F'+1)} \\ \times \begin{Bmatrix} J & F & I \\ F' & J' & 1 \end{Bmatrix} \langle J\|Q_1^{\mathrm{el}}\|J'\rangle\, \delta_{I,I'} \end{aligned} \tag{5}$$

where the symbol in curly brackets denotes a Wigner 6J-symbol. Using equation (5) the relative intensities of the peaks corresponding to the hyperfine components 7/2, 5/2 and 3/2 can be calculated to be (normalized) 4/9, 3/9 and 2/9 respectively.

4 Results

Multiple spectra were recorded of the three transitions in Pd I under various laser power conditions to check for saturation broadening effects. The peaks in the spectra were fitted simultaneously to Lorentzian line profiles using a nonlinear least-squares routine.

In the case of the $4d^{10}\ {}^1S_0 \rightarrow 4d^9 5p\ {}^3P_1$ transition the measured spectrum (Fig. 2a) shows 7 clear peaks, which are assigned (in order of increasing energy) to ^{105}Pd ($F = 7/2$), ^{110}Pd, ^{108}Pd, ^{106}Pd, ^{104}Pd, ^{105}Pd ($F = 5/2$) and ^{105}Pd ($F = 3/2$). ^{102}Pd was not visible in the spectrum, because it coincided with the larger ^{105}Pd ($F = 5/2$) peak. The hyperfine components could be assigned unambiguously by applying a magnetic field and counting the number of m-components of the $F = 3/2$ state.

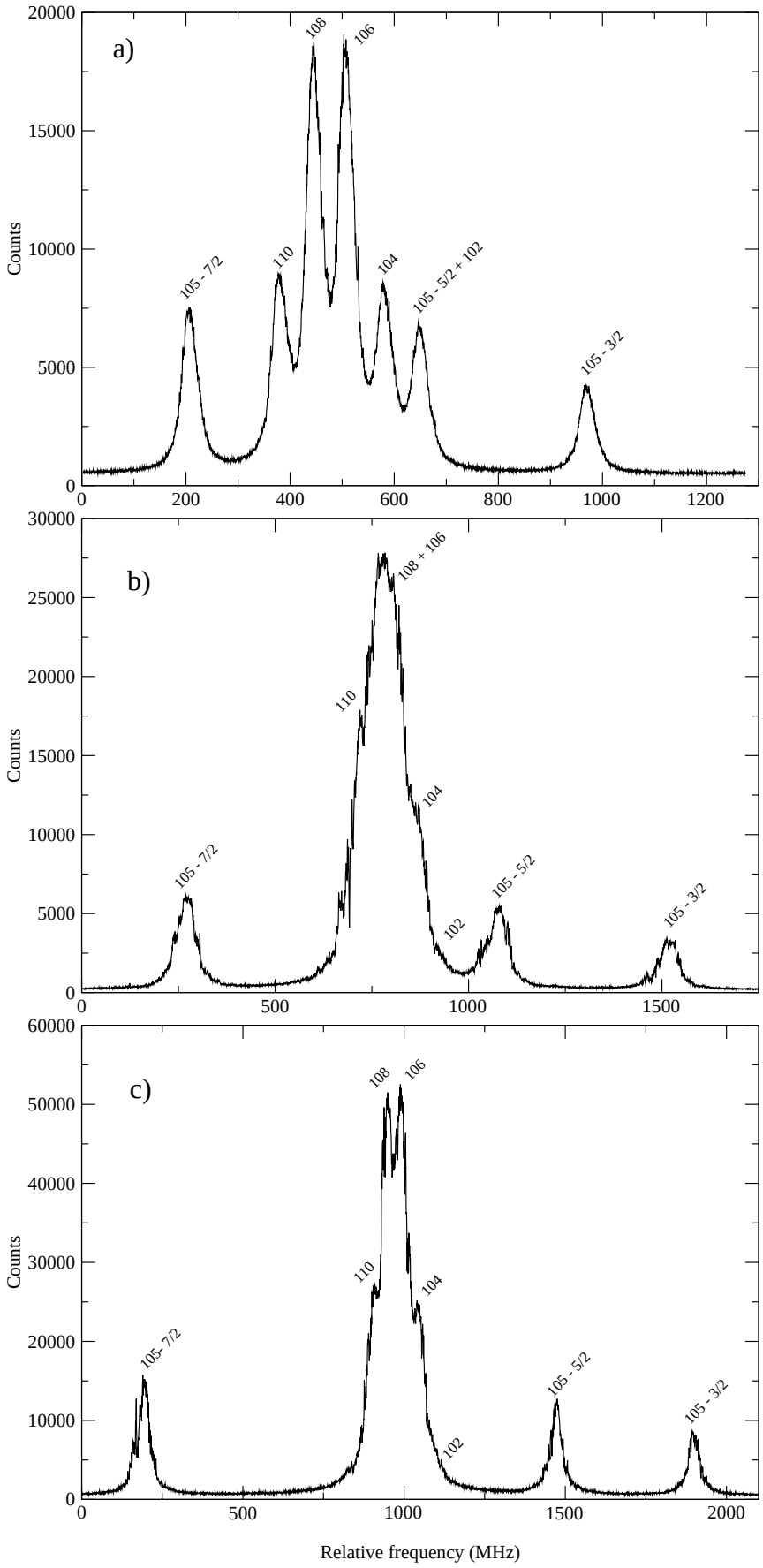

Fig. 2. Examples of LIF measurements on the (a) $4d^{10}\ {}^1\mathrm{S}_0 \rightarrow 4d^9 5p\ {}^3\mathrm{P}_1$, (b) $4d^{10}\ {}^1\mathrm{S}_0 \rightarrow 4d^9 5p\ {}^3\mathrm{D}_1$ and (c) $4d^{10}\ {}^1\mathrm{S}_0 \rightarrow 4d^9 5p\ {}^1\mathrm{P}_1$ transitions.

Table 1. Isotope shifts in Pd I transitions.

Transition	Energy level (cm^{-1})	Isotope shift (MHz)		
		110−108	108−106	106−104
$4d^{10}\ ^1S_0 \rightarrow 4d^9 5p\ ^3P_1$	36 180.694	66.4 (1.3)	62.7 (0.5)	73.5 (0.5)
$4d^{10}\ ^1S_0 \rightarrow 4d^9 5p\ ^3D_1$	40 368.828	47 (9)	45 (6)	59 (7)
$4d^{10}\ ^1S_0 \rightarrow 4d^9 5p\ ^1P_1$	40 838.881	48 (3)	44 (3)	54 (3)

Table 2. Hyperfine splittings, A and B constants and lifetimes of Pd I states.

Transition	Hyperfine splitting (MHz)		A (MHz)	B(MHz)	τ (ns)
	105 (7/2)−105 (5/2)	105 (5/2)−105 (3/2)			
$4d^9 5p\ ^3P_1$	442 (2)	320.3 (0.8)	–126.9 (0.6)	2.0 (0.9)	5.2 (0.3)
Previous work [5]	319	543	–133 (2)	140 (30)	7.46 (0.32)
$4d^9 5p\ ^3D_1$	805 (16)	446 (4)	–212 (5)	–57 (8)	3.1 (0.2)
$4d^9 5p\ ^1P_1$	1281 (4)	426 (3)	–300 (1)	–217.5 (0.8)	4.3 (0.2)

Examples of recorded spectra are shown in Figure 2. The areas under the peaks are in good agreement with the relative natural abundances of the Pd isotopes. Also, the relative intensities of the hyperfine components agree well with the theoretical values given in Section 3.

For the $4d^{10}\ ^1S_0 \rightarrow 4d^9 5p\ ^3D_1$ and the $4d^{10}\ ^1S_0 \rightarrow 4d^9 5p\ ^1P_1$ transitions the same assignment could be made, with the exception that here the ^{102}Pd resonance is not covered by a ^{105}Pd hyperfine component. The isotope shifts in the studied transitions are collected in Table 1. From a King plot analysis [7] it follows straightforwardly that the magnitude of the field shift in these transitions is of the order of 10 MHz. This agrees with the expectation that the field shift in a $d \rightarrow p$ transition is small.

For all transitions, the measured energy of the levels are in good agreement with existing data [1]. The width of the peaks could also be determined from the recorded spectra using the representative ^{105}Pd ($F = 3/2$) peak, which is well isolated from the rest of the peaks. For the $4d^9 5p\ ^3P_1$ this resulted in a full width at half maximum of

$$\Gamma = 36.0\,(1.0)\ \text{MHz}.$$

After correction for the residual Doppler broadening this leads to a lifetime τ of

$$\tau = 5.2\,(0.3)\ \text{ns}.$$

For the $4d^9 5p\ ^3D_1$ and the $4d^9 5p\ ^1P_1$ the lifetimes are, respectively, 3.1(0.2) ns and 4.3(0.2) ns.

Energy splittings due to hyperfine structure are collected in Table 2. Using equations (4) the hyperfine structure constants A and B were derived from these splittings. The resulting values for A and B are given in Table 2 as well, along with the lifetimes of the states. The values for the lifetime and the hyperfine energy splitting for the $^3P_1$level deviate considerably from those reported by Liening [5], while the energy intervals are reversed. As a result, the A and B constants for this level deviate from Liening's results (see Tab. 2). This deviation is unexplained, but the accuracy of the present experimental data gives confidence that our data are correct.

5 Conclusions

LIF measurements on ground state transitions to the first excited states $4d^9 5p\ ^3P_1$, $^3D_1$ and $^1P_1$ in Pd I have been performed using a high resolution, tunable deep-UV cw laser system with a bandwidth smaller than 3 MHz. Hyperfine structure, isotope shifts and lifetimes of the excited states have been measured with high accuracy.

References

1. R. Engleman *et al.*, Phys. Scripta **57**, 345 (1998).
2. A. Steudel, Z. Phys. **132**, 429 (1952).
3. P.E.G. Baird, Proc. R. Soc. Lond. A **351**, 267 (1976).
4. E. Kümmel *et al.*, Z. Phys. D **25**, 161 (1993).
5. H. Liening, Z. Phys. **266**, 287 (1974).
6. T.W. Hänsch, B. Couillaud, Opt. Commun. **35**, 441 (1980).
7. W.H. King, *Isotope Shifts in Atomic Spectra* (Plenum Press, New York, 1984).
8. G.K. Woodgate, *Elementary Atomic Structure*, 2nd edn. (Oxford University Press, 1989).
9. M. Mizushima, *Quantum Mechanics of Atomic Spectra and Atomic Structure* (W.A. Benjamin, Inc., New York, 1970).